SYNTHESIS, MOLECULAR MODELLING AND CHOLINE ESTERASE ENZYME INHIBITORY ACTIVITY OF NOVEL ENAMINONE DERIVATIVES OF SULFONAMIDES

Mashooq A. Bhat[1*], Burak Tüzün[2], Ismail Koyuncu[3], Ebru Temiz[4], Parham Taslimi[5], Ahmed M. Naglah[1], Mohamed A. Al-Omar[1] and Hurija Džudžević-Čančar[6]

[1]Department of Pharmaceutical Chemistry, College of Pharmacy, King Saud University, Riyadh 11451, Saudi Arabia
[2]Plant and Animal Production Department, Technical Sciences Vocational School of Sivas, Sivas Cumhuriyet University, Sivas, Turkey
[3]Department of Medical Biochemistry, Faculty of Medicine, Harran University, Sanliurfa 63290, Turkey
[4]Program of Medical Promotion and Marketing, Health Services Vocational School, Harran University, Sanliurfa 63300, Turkey
[5]Department of Biotechnology, Faculty of Science, Bartin University, 74100 Bartin, Turkey
[6]Department of Chemistry in Pharmacy, University of Sarajevo - Faculty of Pharmacy, 71000 Sarajevo, Bosnia and Herzegovina

ABSTRACT. The enaminone derivatives of sulfonamides (**1–11**) were obtained in good yield and high purity. Choline esterase (ChE) inhibitory activities of the novel compounds against AChE and BChE were determined by Ellman's method. Ki values of compounds for AChE and BChE enzymes were obtained in the ranges of 14.28-160.17 µM, and 8.30-324.27 µM, respectively. Compound, **9** presented good activity towards AChE and BChE with Ki values of 14.28 µM and 8.30 µM, respectively. Compounds **2** and **10** were found to be the most potent compounds showing cytotoxic effect (IC_{50} = 71.54 µg/mL and IC_{50} = 83.59 µg/mL), respectively, on lung cancer cell line (A549) and normal cells (Beas-2B) (IC_{50} = 164.62 µg/mL and IC_{50} = 155.64 µg/mL), respectively. The compounds have interacted with various proteins like AChE enzyme protein (PDB ID: 4M0E) and BChE enzyme protein (PDB ID: 5NN0). Finally, ADME/T analysis was performed to predict the movements of molecules in human metabolism.

KEY WORDS: Sulfonamides, Enaminone, Enzyme inhibition, Molecular docking

INTRODUCTION

Enaminones are enamines of β-dicarbonyl compounds. They have been used as building blocks for novel drug candidates. The enaminone-containing analogs have shown activity including antibacterial [1], anti-inflammatory [2], antitubercular [3], anticonvulsants [4], antitumor [5], antifungal [6], and antidepressant agents [7].

Sulfonamide drugs were the first antibiotics to be used systemically and paved the new antibiotic revolution in medicine. Nevertheless, antibiotics are not the only function of sulfonamides. The sulfonamide derivatives have been used in various biological applications [8-11]. Sulfonamides are found to form hydrogen bonds as well as interact with unipolar environments within proteins. Therefore, it is strongly foresight that new entities can be developed easily to improve the available machinery helpful in the fight against new and emerging diseases.

There are two different kinds of ChEs at the neuronal level: acetylcholinesterase (AChE) and butyrylcholinesterase (BChE). In a healthy brain, AChE activity predominates (80%), with BChE

_____

acting as a supporter. AChE levels in the brain, however, drop to about 60% of normal levels as the disease progresses, whereas BChE levels rise to 120% of normal levels, indicating that the latter may play a significant role in the more severe forms of the disease and offer a potential therapeutic target for some disease [12, 13].

Recent studies show that theoretical calculations become very important in many stages, from synthesis and characterization to activity comparison. There are many programs used for these stages. Gaussian software and Maestro Schrödinger are the most well-known among these programs [14, 15]. The chemical properties of the molecules were examined with the Gaussian software program, which used this program to calculate at the B3LYP, HF, and M06-2X levels with the 6-31++g(d,p) basis sets [16, 17]. On the other hand, their activities were compared against various proteins such as AChE enzyme protein (PDB ID: 4M0E), and BChE enzyme protein (PDB ID: 5NN0), using the Maestro Schrödinger program [18]. Finally, ADME/T calculations were made to predict the molecule's action, response, and movement in human metabolism.

In continuation of our research on enaminones, herein we have synthesized a series of compounds containing the combined pharmacophore, both the enaminone and sulfonamide moiety (**1-11**) [19]. Afterward, the activities of the molecules against AChE and BChE enzymes were examined. Quantum chemical parameters were calculated with the Gaussian package program to compare the theoretical activity of molecules. Activity calculations were made against AChE enzyme protein (PDB ID: 4M0E) and BChE enzyme protein (PDB ID: 5NN0) with molecular docking calculations. Finally, ADMET analysis was carried out to predict the movement of molecules.

RESULTS AND DISCUSSION

Treatment of differently substituted acetophenones (**1a-f**) under solvent-free conditions afforded orange to red color crystalline products as enaminones (**2a-f**). The reaction of enaminone (**2a-f**) with different sulfonamides was performed in the presence of glacial acetic acid to obtain enaminone derivatives of sulfonamides [20]. Compounds (**1-6**), (**7-8**), **9**, and (**10-11**) were obtained by reacting enaminones with sulfadiazine, sulfametrol, sulfamoxole, and sulfanilamide, respectively in Scheme 1.

The structures of the enaminones were identified spectroscopically. The enaminones presented two singlets due to *N,N* dimethyl protons and two doublets due to ethylenic protons. The multiplet was also obtained at the aromatic region in addition to methoxy protons. The methoxy protons appeared as singlets in the range of δ 3.70-3.89 ppm in ^{1}H NMR. The aromatic protons appeared as multiplet and were present in the range of δ 6.01-8.97 ppm. The NH protons appeared as broad singlets with different values ranging from δ 8.14-11.98 ppm. The SO_2NH proton also appeared as a singlet ranging from δ 7.04-12.06 ppm. ^{13}C NMR of all compounds agreed with their structures. All the structures of the synthesized compounds were confirmed by ^{1}H NMR and ^{13}C NMR.

Enzyme study

The K_i values of the test compounds demonstrated that the most active compound against AChE and BChE was compound **9** (AChE, K_i = 14.28 ± 2.64 µM; BChE, K_i = 8.30 ± 1.17 µM) (Table 1). Also, for AChE, IC_{50} values of compounds were studied in the following order: **9** (16.13 µM, r^2: 0.932) < **8** (34.25 µM, r^2: 0.919) < **5** (43.84 µM, r^2: 0.952) < **1** (48.57 µM, r^2: 0.943) < **4** (50.16 µM, r^2: 0.925) < TAC (151.20 µM, r^2: 0.904).

The third most potent compound among the synthesized derivatives against AChE was derivative **5** with Ki: 39.28 µM. In this work, the second and third most potent compounds among the synthesized derivatives against BChE were **9** and **7** with Ki: 8.30 ± 1.17 and 10.56 ± 1.05 µM. Additionally, the weak inhibitors for both enzymes were **10** and **11** compounds with Ki values of 160.17 ± 11.21 and 105.04 ± 8.05 µM against AChE, and 214.27 ± 18.81 and 324.14 ± 24.56 µM against BChE, respectively in Figure 1.
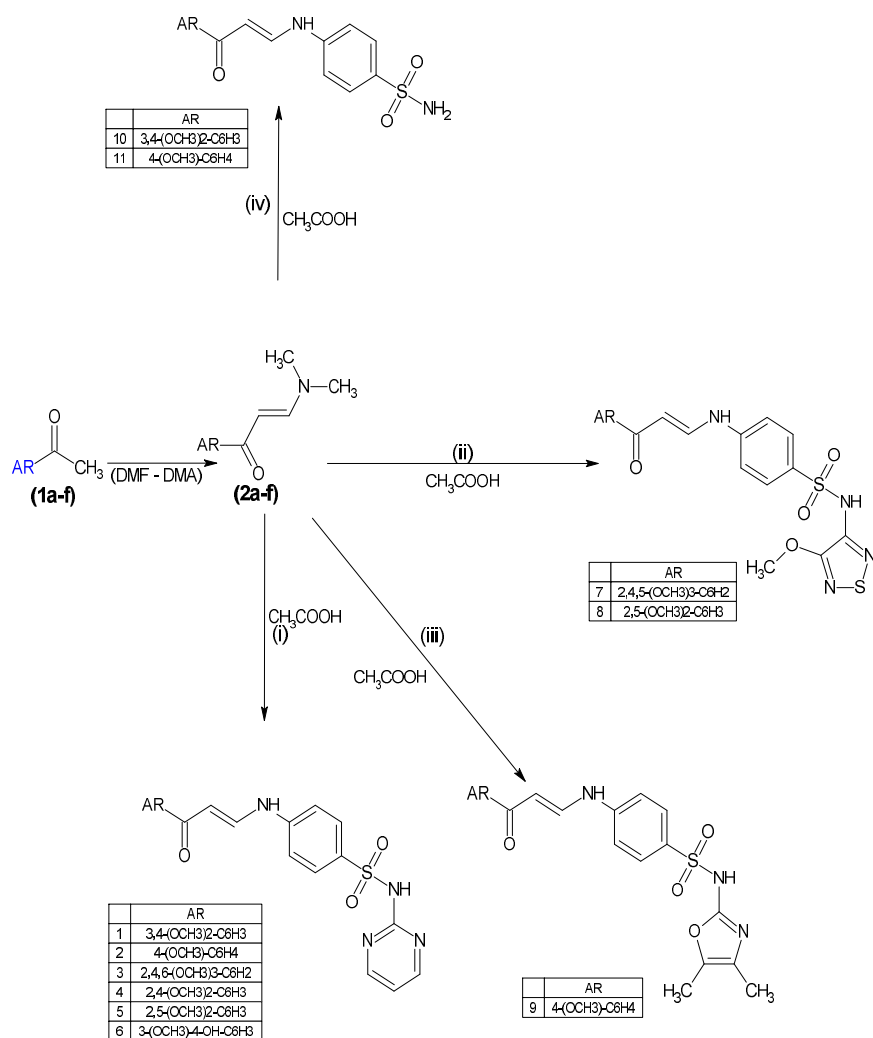
Scheme 1. Reaction scheme of synthesis of enaminone-derived sulfonamides (**1-11**).
(i) sulfadiazine; (ii) sulfametrol; (iii) sulfamoxole; (iv) sulfanilamide.

Table 1. The enzyme inhibition results of compounds (**1-11**) against AChE and BChE. *Tacrine values taken
from these references.

| Compounds	IC$_{50}$ (µM)				Ki(µM)	
	AChE	r^2	BChE	r^2	AChE	BChE
1	48.57	0.943	44.68	0.917	47.26±5.74	38.05±6.27
2	53.42	0.987	42.60	0.915	50.48±6.11	39.84±7.88
3	98.33	0.985	91.52	0.980	95.06±8.76	87.15±11.18
4	50.16	0.925	48.38	0.998	46.24±4.54	39.32±5.44
5	43.84	0.952	39.02	0.941	39.28±5.41	34.31±4.67
6	98.21	0.936	35.81	0.918	97.46±9.71	31.24±3.78
7	64.08	0.989	11.67	0.954	58.17±6.70	10.56±1.05
8	34.25	0.919	27.58	0.971	31.60±3.34	23.27±2.84
9	16.13	0.932	10.07	0.945	14.28±2.64	8.30±1.17
10	176.85	0.986	229.18	0.936	160.17±11.21	214.27±18.81
11	113.03	0.974	340.23	0.918	105.04±8.05	324.14±24.56
Tacrine*	151.20	0.904	192.72	0.974	± 10.83	188.70± 24.18
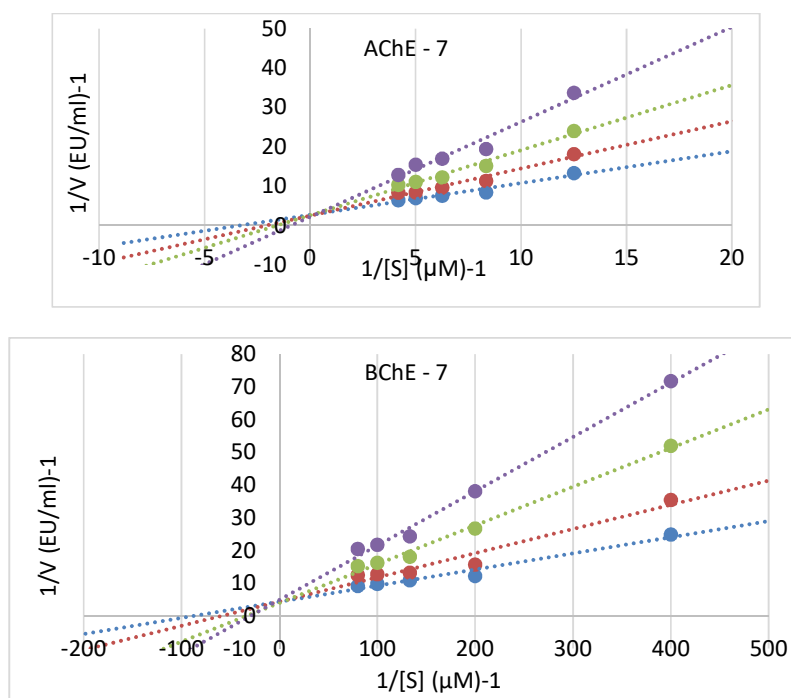
Figure 1. Lineweaver-Burk graphs of best inhibitors.

Proliferation inhibition of lung cancer cells

The IC$_{50}$ values were calculated by treating all molecules at doses of 0-200 µg/mL for 24 hours in
lung cancer (A549) and lung normal (Beas-2B) cell lines (Table 2).

Table 2. Cytotoxic effects of (1-11) on A549 and Beas-2B cell lines (IC$_{50}$).

Compounds	IC$_{50}$ (µM/mL)	
	A549	BEAS-2B
1	0.35	0.40
2	0.17	0.40
3	1.31	0.45
4	0.79	0.25
5	1.08	0.38
6	0.29	0.38
7	0.38	0.50
8	0.42	0.29
9	0.49	0.33
10	0.23	0.42
11	0.36	0.48

The 2 and 10 were found to be highly active compounds showing cytotoxic effect (IC$_{50}$: 0.17 µM/mL; IC$_{50}$: 0.23 µM/mL) on lung cancer (A549). The IC$_{50}$ value was calculated using the GraphPad Prism 9 program (Figure 2).
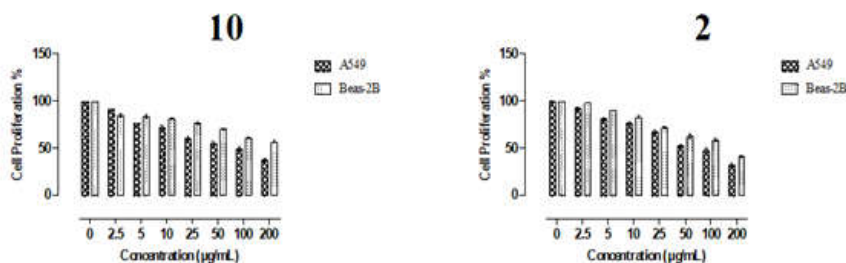

Figure 2. Evaluation of cytotoxic effects of 10 and 2 on A549 and Beas-2B cell line by MTT assay. All data are expressed as the mean ± SD from three independent experiments. The IC$_{50}$ value was calculated using the GraphPad Prism 9 program.

Effect on the morphology of lung cancer cells

Light microscopy evaluation was performed to observe the cell's morphological changes. In A549 cells treated with 10 and 2, both cellular and nuclear morphologic changes were detected. In lung cancer cells, it was observed that the morphology of the cells has deteriorated and cell numbers were decreased, in proportion to the IC$_{50}$ dose compared to the negative group (Figure 3).
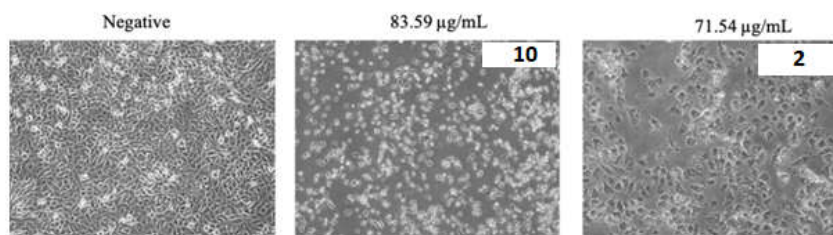

Figure 3. Morphological observation of A549 with the administration of 10 and 2.

Theoretical calculation

With theoretical calculations, it is possible to have a lot of information about the molecule. Among these theoretical calculations, one of the most widely used is the Gaussian software program, which gives important information about chemical properties of molecules. To compare the activities of molecules, numerical values of two parameters of molecules are used, which are HOMO and LUMO. The HOMO parameter of molecules shows the ability of molecules to donate electrons. It is known that the activity of the molecule with the most positive numerical value of this parameter is the highest [21].

On the other hand, the LUMO parameter of the molecules shows the electron-accepting capacity of the molecule, which shows that the activity of the molecule with the most negative numerical value of this parameter is higher than the other molecules [22, 23]. The numerical value of these two parameters allows the interpretation of the activity of molecules. Apart from these two parameters, it is predicted that the activity of the molecule with the smallest numerical value of the ΔE parameter of the molecules is higher than the other molecules.

Apart from these parameters, another calculated parameter is electronegativity. The electronegativity parameter shows the strength of the atoms in the molecule to attract the bond electrons. As the numerical value of this parameter increases, its electronegative value will increase, which will decrease the activity of the molecule [24]. Several parameters are calculated, and each parameter gives information about the different properties of the molecules. Among these, four parameters are more important than the others. The visuals of these parameters are shown in Figure 4.
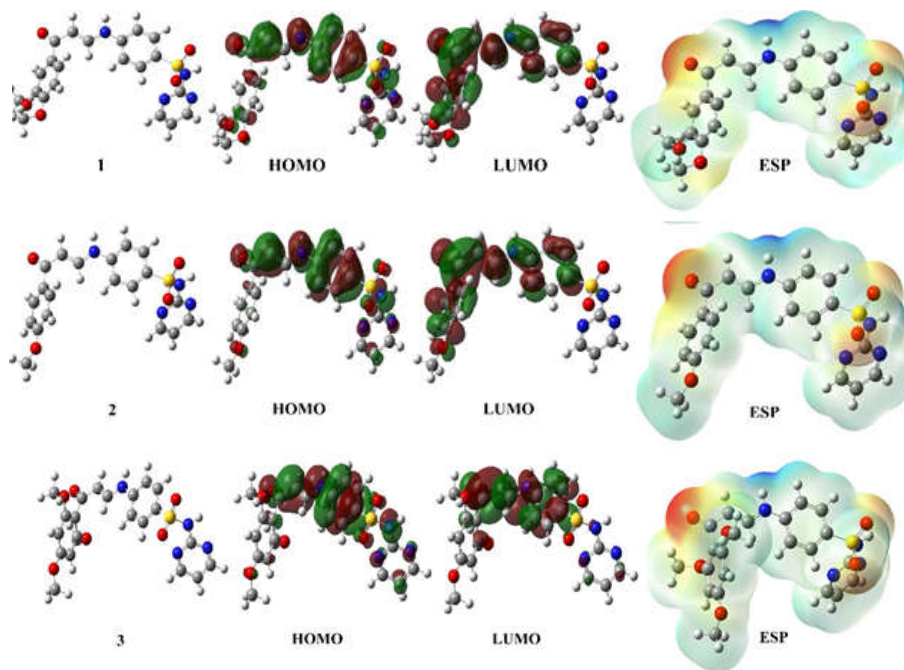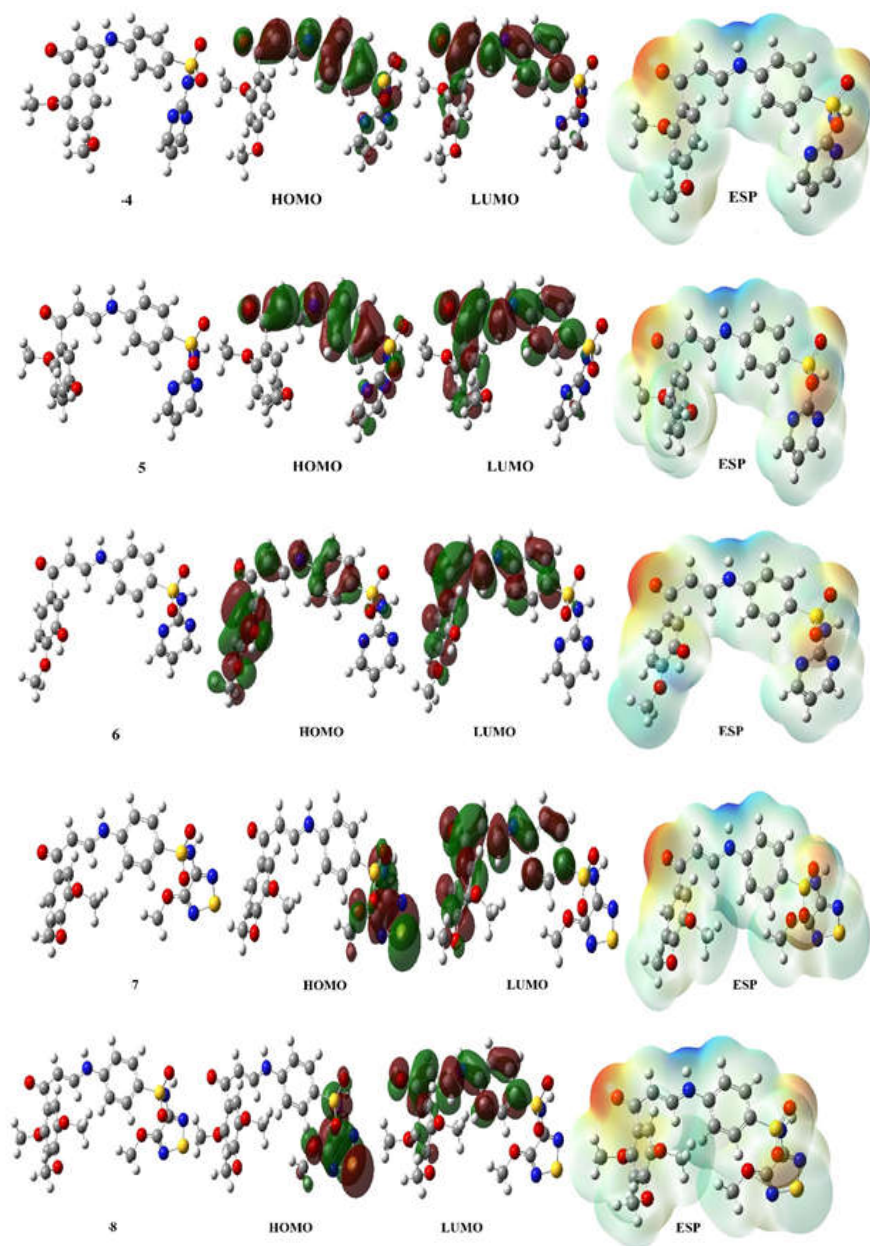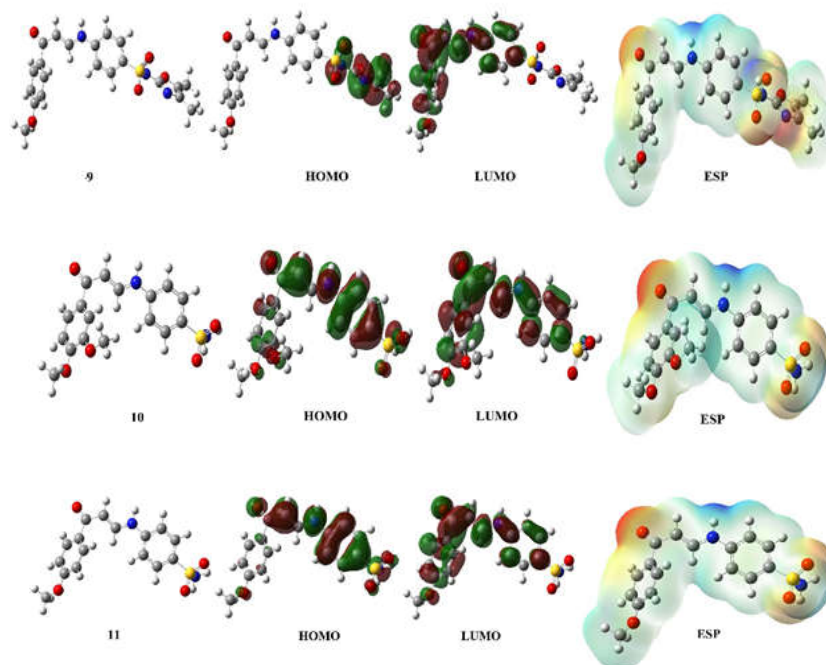
Figure 4. Representations of optimizing structure, HOMO, LUMO, and ESP of (**1-11**).

There are four different pictures in these images, the first of which is the picture of the optimized structure of molecules. The next two pictures represent the HOMO and LUMO orbitals of the molecules. In the last picture, the electrostatic potential (ESP) of the molecules has been provided. In this picture, there is a color scale from blue to red, which shows the regions with the lowest electron density. The red color indicates the regions with the highest electron density [25, 26].

It is possible to make molecular docking calculations to compare the activities of the studied molecules against biological materials. By these calculations, it is made to predict the active sites of molecules and to examine the interactions of molecules with proteins, which are formed by biological materials [27]. During molecular docking calculations, the most important factor determining the activities of molecules is the interactions between molecules and proteins. Molecules try to inhibit proteins as a result of these interactions. For this reason, the chemical interactions between the molecule and the protein have gained great importance, which are hydrogen bonds, polar and hydrophobic interactions, π-π interaction [28, 29]. It has been observed that as these chemical interactions increase, the activities of the molecules increase.

When the interaction between the compound **9** and the AChE enzyme protein is examined, the benzene ring in the center of the compound **9** creates a Pi-Pi stacking interaction with the TRP 286 protein. The oxygen atom attached to the carbonyl carbon in the same molecule makes a hydrogen bond interaction with the PHE 295 protein. It is observed that the methoxy benzene ring in the same molecule forms Pi-Pi stacking interactions with TYR 341 and TYR 124 proteins (Figure 5).

When the interaction between the compound **9** and the BChE enzyme protein is examined, it is seen that the 4,5-dimethyl-2,3dihydrooxazole ring in the compound **9** creates Pi-Pi stacking interactions with the PHE 329 and TRP 231 proteins (Figure 6).

As a result of the MM-GBSA calculations, the binding free energy values of the molecules were calculated by Maestro. It was observed that the binding free energy value of compound **10** was found to be with a numerical value of -27.51. However, there are many interactions between molecules and proteins. These interactions are coulomb, covalent, H bond, lipophilic, packaging, Solv GB and vdW interactions [30]. Each interaction was found to be of greater importance in different molecules. For example, Coulomb and vdw (van der Waals) interactions are more common in the interaction between the compound **10** and the protein.
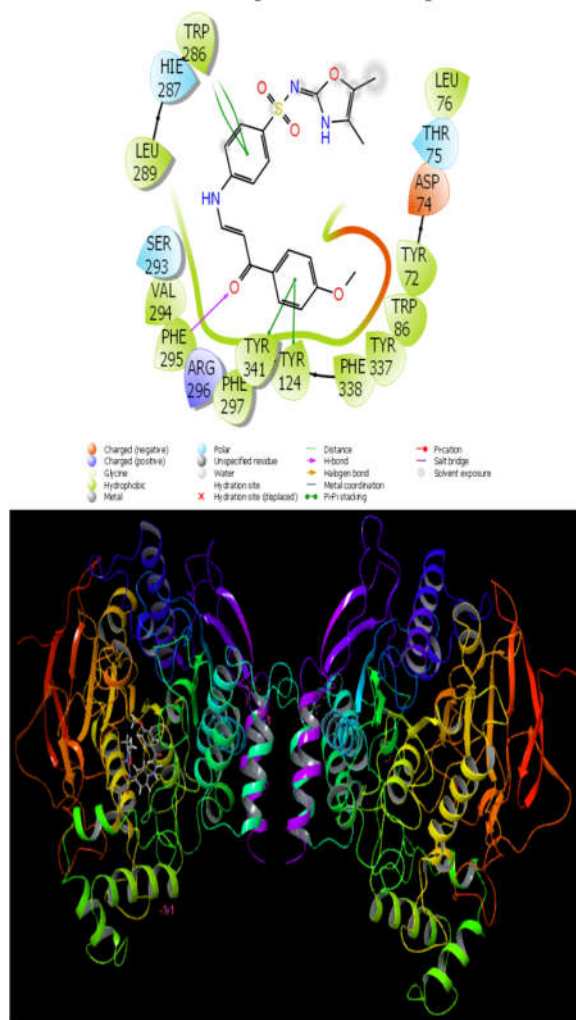

Figure 5. Presentation interactions of compound **9** with AChE enzyme protein.

As a result of the calculations, the activities of the molecules against various proteins are compared. For this comparison, the docking score parameter is made according to its numerical value; the most negative numerical value of this parameter has the highest activity. Although many parameters except the docking score parameter, are calculated in the molecular docking calculations, the parameter that affects the activity is quite limited. Parameters such as Glide ligand efficiency, Glide Hbond, Glide evdw, and Glide ecoul give numerical values obtained on the interaction between molecules and proteins [31]. On the other hand, the four calculated parameters, Glide emodel, Glide energy, Glide einternal, and Glide posenum, give the numerical values obtained on the pose formed as a result of the interaction [32].
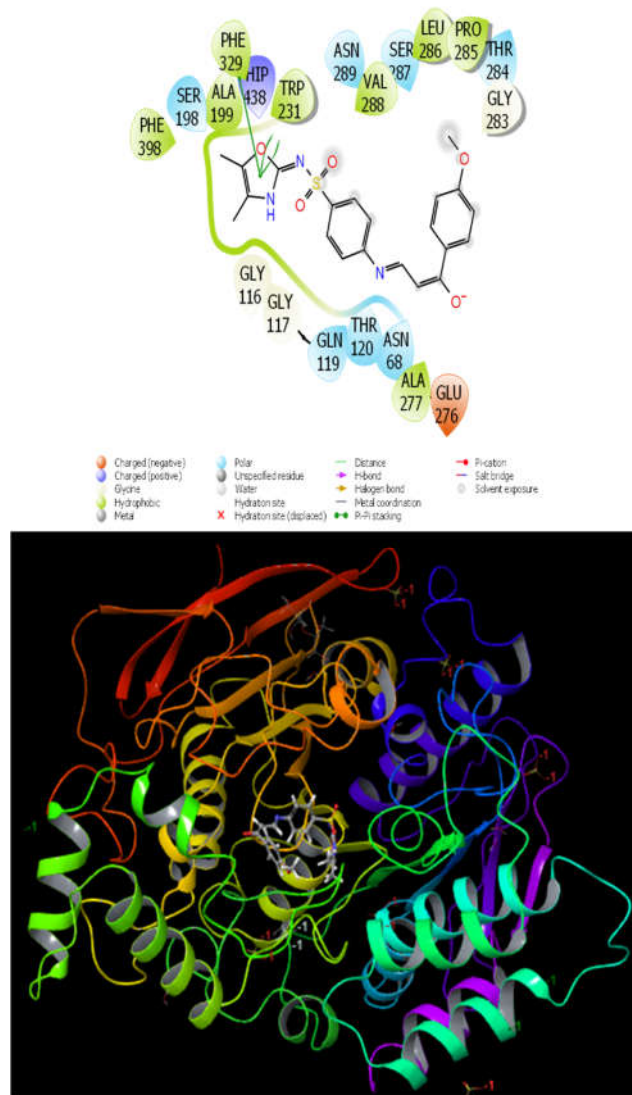

Figure 6. Presentation interactions of **9** with BChE enzyme protein.

After comparing the activities of compounds (**1-11**) against various proteins, it has been theoretically tested that these molecules can be used as drugs for human metabolism. ADME/T analysis was performed. With this analysis, the movements of molecules in human metabolism are predicted. The entry of the molecule into human metabolism includes many processes including movements in metabolism and excretion from metabolism, which are called ADME/T for short, known as Absorption, Distribution, Metabolism, Excretion, and Toxicity. This analysis is divided into two. Firstly, the chemical properties of the molecules in the first part and the biological properties of the molecules in the second part are examined.

Many parameters are examined in the chemical properties of molecules, such as mol_MW (mole mass of molecules), dipole (dipole moment), SASA (solvent accessible surface area), volume (molecule volume), donor HB and accept HB (number of hydrogen bonds that a molecule receives and gives off). On the other hand, many parameters examine the biological properties of molecules, which are QPlog HERG (Predicted IC_{50} value for blockage of HERG K^+ channels), QPPCaco and QPPMDCK (blood-brain and blood-bowel barriers), QPlog Kp (Predicted skin permeability), QPlogKhsa (Prediction of binding to human serum albumin), and Human Oral Absorption (Predicted qualitative human oral absorption) [33]. Apart from these, there are two parameters such as rule of five [34, 35] and rule of three [36], that examine the drug feasibility of molecules. The numerical value of all these calculated parameters showed that the molecules can be used for human metabolism.

EXPERIMENTAL

Chemical and instruments

All the solvents were obtained from (Merck). Thin layer chromatography (TLC) was performed on Silica gel $60F_{254}$ (Merck). Perkin Elmer FT-IR spectrophotometer (PerkinElmer Inc.) was used for FT-IR spectroscopy. Gallenkamp melting point apparatus was used for melting point determination. ^1H and ^{13}C NMR spectra of the compounds were performed on Bruker NMR 500/700 MHz (Bruker) respectively. Mass spectra of compounds were performed on Agilent triple quadrupole 6410 TQ GC/MS equipped with ESI (electrospray ionization). The elemental analysis of the compounds was performed by CHN Elementar (Analysensysteme GmbH).

General procedure for the preparation of enaminone intermediate (*2 a-f*)

Compounds (**2a-f**) were prepared according to the reported procedure [37].

General procedure for the preparation of enaminone sulfonamide derivative (**1-11**)

The enaminone (**2a-f**) (0.1 mol) was added to a hot stirred solution of sulfonamide (0.1 mol) in glacial acetic acid (15 mL) and was refluxed for 4 h. After the completion of the reaction, which was confirmed by thin-layer chromatography. The reaction was stopped by adding cold water to the reaction mixture. The compound was precipitated and was collected by filtration. The crude product was washed several times with cold water and methanol. The product was dried and recrystallized from ethanol to afford the final product.

4-[(3-(3,4-Dimethoxyphenyl)-3-oxoprop-1-en-1-yl]-4-amino-N-(pyrimidin-2-yl)   benzene-1-sulfonamide (1). Yield: 65%; m. p.: 265-267 °C; FT-IR (KBr) v cm^{-1}: 2911 (NH str.), 1679 (C=O), 1542 (C=N), 1336, 1156 (SO$_2$NH); ^1H NMR (500 MHz, DMSO–d$_6$) δ (ppm): 3.84 (6H, s, 2 ×OCH$_3$), 6.24 (1/2 H, d, Ar-H, J = 10 Hz), 6.57 (1/2 H, d, Ar-H, J = 15 Hz), 7.06 (2H, s, ArH), 7.27-7.28 (1H, d, SO$_2$NH, J = 5 Hz), 7.45 (7H, m, Ar-H), 10.33 (d, ½ H, NH, D$_2$O exchange), J = 15 Hz), 10.02 (d, ½ H, NH, D$_2$O exchange), J = 10 Hz); MS: *m/z* = 440.47 [M]$^+$; analysis: for

$C_{21}H_{20}N_4O_5S$, calcd. C 57.26, H 4.58, N 12.72, S 7.28 %; found C 57.06, H 4.57, N 7.24, S 7.30 %.

4-[3-(4-Methoxyphenyl)-3-oxoprop-1-en-1-yl]-4-amino-N-(pyrimidin-2-yl) benzene-1-sulfon-amide (**2**). Yield: 70%; m. p.: 280-282 °C; FT-IR (KBr) ν cm^{-1}: 2986 (NH str.), 1641 (C=O), 1479 (C=N), 1231, 1153 (SO$_2$NH); ^{1}H NMR (500 MHz, DMSO–d$_6$) δ (ppm): 3.84 (6H, s, 2 ×CH$_3$), 6.21 (1H, d, Ar-H, J = 10 Hz), 6.54 (1H, d, Ar-H, J = 15 Hz), 7.05 (2H, s, Ar-H), 7.27-7.28 (1H, d, SO$_2$NH, J = 5 Hz), 7.46-8.52 (9H, m, Ar-H), 10.33 (d, 1H, NH, D$_2$O exchange), J = 15 Hz), 11.98 (d, 1H, NH, D$_2$O exchange), J = 15 Hz); MS: *m/z* = 410.44 [M]$^+$; analysis: for $C_{20}H_{18}N_4O_4S$, calcd. C 58.53, H 4.42, N 13.65, S 7.81 %; found C 58.72, H 4.43, N 13.60, S 7.80 %.

4-[3-(2,4,6-Trimethoxyphenyl)-3-oxoprop-1-en-1-yl]-4-amino-N-(pyrimidin-2-yl) benzene-1-sulfonamide (**3**). Yield: 65%; m. p.: 270-272 °C; FT-IR (KBr) ν cm^{-1}: 2985 (NH str.), 1686 (C=O), 1589 (C=N), 1334, 1156 (SO$_2$NH); ^{1}H NMR (500 MHz, DMSO–d$_6$) δ (ppm): 3.71-3.89 (9H, s, 3 ×OCH$_3$), 6.27 (1H, d, Ar-H, J = 10 Hz), 6.56 (1H, d, Ar-H, J = 10 Hz), 7.05 (2H, s, Ar-H), 7.27-7.28 (1H, d, SO$_2$NH), 7.87-8.51 (7H, m, Ar-H), 10.73 (d, 1H, NH, D$_2$O exchange), J = 15 Hz); ^{13}C NMR (125.76 MHz, DMSO–d$_6$) δ (ppm): 21.5, 55.8, 91.5, 98.7, 112.5, 114.3, 116.2, 118.4, 129.3, 130.2, 139.9, 153.5, 157.4, 158.7, 166.2, 172.0; MS: *m/z* = 470.49 [M]$^+$; analysis: for $C_{22}H_{22}N_4O_6S$, calcd. C 56.16, H 4.71, N 11.90, S 6.82 %; found C 56.37, H 4.70, N 11. 85, S 6.84%.

4-[3-(2,4-Dimethoxyphenyl)-3-oxoprop-1-en-1-yl]-4-amino-N-(pyrimidin-2-yl) benzene-1-sulfonamide (**4**). Yield: 60%; m. p.: 250-252 °C; FT-IR (KBr) ν cm^{-1}: 2984 (NH str.), 1690 (C=O), 1520 (C=N), 1397, 1154 (SO$_2$NH); ^{1}H NMR (500 MHz, DMSO–d$_6$) δ (ppm): 3.83 (6H, s, 2 ×OCH$_3$), 6.21 (1/2 H, d, Ar-H, J = 10 Hz), 6.49 (1/2 H, d, Ar-H, J = 10 Hz), 6.64 (2H, s, ArH), 7.04 (1H, s, SO$_2$NH), 7.21-8.50 (8H, m, Ar-H), 10.21 (d, ½ H, NH, D$_2$O exchange), J = 10 Hz), 11.89 (d, ½ H, NH, D$_2$O exchange), J = 10 Hz); ^{13}C NMR (125.76 MHz, DMSO–d$_6$) δ (ppm): 21.5, 55.9, 56.2, 99.0, 101.0, 106.3, 112.6, 114.7, 121.8, 130.2, 132.2, 141.3, 142.9, 145.7, 157.4, 158.8, 159.8, 160.0, 163.4, 172.5, 188.1, 190.0; MS: *m/z* = 440.47 [M]$^+$; analysis: for $C_{21}H_{20}N_4O_5S$, calcd. C 57.26, H 4.58, N 12.72, S 7.28%; found C 57.13, H 4.57, N 12.77, S 7.26%.

4-[3-(2,5-Dimethoxyphenyl)-3-oxoprop-1-en-1-yl]-4-amino-N-(pyrimidin-2-yl) benzene-1-sulfonamide (**5**). Yield: 75%; m. p.: 255-257 °C; FT-IR (KBr) ν cm^{-1}: 2979 (NH str.), 1691 (C=O), 1522 (C=N), 1331, 1069 (SO$_2$NH); ^{1}H NMR (500 MHz, DMSO–d$_6$) δ (ppm): 3.78 (6H, s, 2 ×OCH$_3$), 6.34 (1/2 H, d, Ar-H, J = 15 Hz), 6.58 (1/2 H, d, Ar-H, J = 10 Hz), 7.02 (2H, s, ArH), 7.20 (1H, d, SO$_2$NH), 7.46-8.50 (8H, m, Ar-H), 10.31 (d, 1H, NH, D$_2$O exchange), J = 10 Hz), 11.86 (d, 1H, NH, D$_2$O exchange), J = 15 Hz); ^{13}C NMR (125.76 MHz, DMSO–d$_6$) δ (ppm): 21.5, 55.9, 56.7, 100.8, 106.2, 112.6, 114.1, 115.0, 116.1, 130.0, 131.0, 142.4, 143.7, 144.5, 145.4, 151.7, 153.4, 157.4, 158.8, 172.5, 189.7, 190.9; MS: *m/z* = 440.47 [M]$^+$; analysis: for $C_{21}H_{20}N_4O_5S$, calcd. C 57.26, H 4.58, N 12.72, S 7.28%; found C 57.05, H 4.59, N 12.76, S 7.30%.

*4-[3-(3-Methoxy, 4-hydroxyphenyl)-3-oxoprop-1-en-1-yl]- 4-amino-N-(pyrimidin2-yl) benzene-1-sulfonamide (**6**)*. Yield: 70%; m. p.: 245-247 °C; FT-IR (KBr) ν cm^{-1}: 2983 (NH str.), 1692 (C=O), 1583 (C=N), 1321, 1148 (SO$_2$NH); ^{1}H NMR (500 MHz, DMSO–d$_6$) δ (ppm): 3.84 (3H, s, s, Ar-H), 6.01 (1H, s, Ar-H), 6.54 (1H, d, Ar-H, J = 10 Hz), 7.01-7.63 (10 H, m, Ar-H), 8.48 (1H, d, SO$_2$NH), 10.32 (1H, NH, D$_2$O exchange), 11.50 (1H, s, OH, D$_2$O exchange); ^{13}C NMR (125.76 MHz, DMSO–d$_6$) δ (ppm): 112.5, 116.0, 118.6, 125.3, 130.2, 153.4, 157.6, 158.7, 169.5, 172.5; MS: *m/z* = 426.44 [M]$^+$; analysis: for $C_{20}H_{18}N_4O_5S$, calcd. C 56.33, H 4.25, N 13.14, S 7.52%; found C 56.55, H 4.24, N 13.18, S 7.50%.

4-[3-(2,4,5-Trimethoxyphenyl)-3-oxoprop-1-en-1-yl]-4-amino-N-(4-methoxy-1,2,5thiadiazol-3-yl) benzene-1-sulfonamide (7). Yield: 72%; m. p.: 273-275 °C; FT-IR (KBr) ν cm⁻¹: 2981 (NH str.), 1690 (C=O), 1521 (C=N), 1336, 1069 (SO$_2$NH); ¹H NMR (500 MHz, DMSO–d$_6$) δ (ppm): 3.79 (12H, s, 4×OCH$_3$), 6.48 (1H, s, Ar-H), 6.81 (1H, s, Ar-H), 7.11-8.36 (6H, m, Ar-H)., 9.42 (1H, s, NH, D$_2$O exchange), 10.33 (1H, s, SO$_2$NH, D$_2$O exchange); ¹³C NMR (125.76 MHz, DMSO–d$_6$) δ (ppm): 21.5, 24.5, 49.0, 56.1, 58.2, 111.3, 112.7, 115.1, 118.8, 129.0, 140.1, 143.8, 155.7, 169.5, 172.5; MS: *m/z* = 506.55 [M]⁺; analysis: for C$_{21}$H$_{22}$N$_4$O$_7$S$_2$, calcd. C 49.79, H 4.38, N 11.06, S 12.66 %; found C 49.95, H 4.39, N 11.10, S 12.68%.

4-[3-(2,5-Dimethoxyphenyl)-3-oxoprop-1-en-1-yl]-4-amino-N-(4-methoxy-1,2,5thiadiazol-3-yl) benzene-1-sulfonamide (8). Yield: 70%; m. p.: 255-257°C; FT-IR (KBr) ν cm⁻¹: 2984 (NH str.), 1690 (C=O), 1521 (C=N), 1394, 1066 (SO$_2$NH); ¹H NMR (500 MHz, DMSO–d$_6$) δ (ppm): 3.70 (3H, s, OCH$_3$), 3.79 (3H, s, OCH$_3$), 3.89 (3H, s, OCH$_3$), 6.80 (1H, s, Ar-H), 6.82 (1H, s, Ar-H), 7.02-8.97 (7H, m, Ar-H), 9.52 (1H, s, NH, D$_2$O exchange), 10.30 (1H, s, SO$_2$NH, D$_2$O exchange); ¹³C NMR (125.76 MHz, DMSO–d$_6$) δ (ppm): 56.0, 56.2, 56.7, 113.0, 114.9, 115.2, 117.0, 118.9, 120.7, 121.5, 125.4, 126.0, 131.4, 136.6, 148.0, 149.6, 152.8, 153.8, 155.2, 157.7, 189.71; MS: *m/z* = 476.52 [M]⁺; analysis: for C$_{20}$H$_{20}$N$_4$O$_6$S$_2$, calcd. C 50.41, H 4.23, N 11.76, S 13.46 %; found C 50.22, H 4.24, N 11.71, S 13.44%.

4-[3-(4-Methoxyphenyl)-3-oxoprop-1-en-1-yl]-4-amino-N-(4,5-dimethyl-1,3oxazol-2-yl) benzene -1-sulfonamide (9). Yield: 65%; m. p.270-272 °C; FT-IR (KBr) ν cm⁻¹: 2980 (NH str.), 1628 (C=O), 1529 (C=N), 1236, 1156 (SO$_2$NH); ¹H NMR (500 MHz, DMSO–d$_6$) δ (ppm): 3.40 (3H, s, OCH$_3$), 3.83 (6H, s, 2×CH$_3$), 6.20 (1H, s, Ar-H), 6.54 (1H, s, Ar-H), 7.03-7.98 (8H, m, Ar-H), 10.28 (1H, s, NH, D$_2$O exchange), 12.0 (1H, s, SO$_2$NH, D$_2$O exchange); ¹³C NMR (125.76 MHz, DMSO–d$_6$) δ (ppm): 8.2, 9.4, 55.8, 95.0, 99.7, 114.2, 115.2, 116.1, 128.3, 131.5, 132.1, 136.2, 136.3, 137.5, 142.9, 143.5, 144.5, 155.5, 162.6, 162.8, 186.7, 189.5; MS: *m/z* = 427.47 [M]⁺; analysis: for C$_{21}$H$_{21}$N$_3$O$_5$S, calcd. C 59.00, H 4.95, N 9.83, S 7.50 %; found C 59.22, H 4.94, N 9.88, S 7.52%.

4-{[3-(3,4-Dimethoxyphenyl)-3-oxoprop-1-en-1-yl]amino}benzene-1sulfonamide (10). Yield: 80%; m. p. 250-252 °C; FT-IR (KBr), ν cm⁻¹: 2900 (NH), 1600 (C=N), 1100 (SO$_2$);¹H NMR (500 MHz, DMSO–d$_6$) δ (ppm): 3.85 (6H, s, 2×OCH$_3$), 6.25 (1H, d, Ar-H, *J* = 10 Hz), 6.59 (1H, d, Ar-H, *J* = 10 Hz), 7.05-7.79 (7H, m, Ar-H), 8.14 (1H, s, NH, D$_2$O exchange), 10.30 (1H, d, NH, D$_2$O exchange), 12.06 (1H, d, NH, D$_2$O exchange); MS: *m/z* = 362.40 [M]⁺; analysis: for C$_{17}$H$_{18}$N$_2$O$_5$S, calcd. C 56.34, H 5.01, N 7.73, S 8.85%; found C 56.36, H 5.02, N 7.70, S 8.83%.

4-{[3-(4-Methoxyphenyl)-3-oxoprop-1-en-1-yl] amino} benzene-1-sulfonamide (11). Yield: 80%; m. p. 260-262 °C; FT-IR (KBr), ν cm⁻¹: 3000 (NH), 1650 (C=O), 1150 (SO$_2$); ¹H NMR (500 MHz, DMSO–d$_6$) δ (ppm): 3.84 (3H, s, OCH$_3$), 6.21 (1H, d, Ar-H, *J* = 10 Hz), 6.56 (1H, d, Ar-H, *J* = 10 Hz), 7.04-7.99 (8H, m, Ar-H), 8.15 (1H, s, NH, D$_2$O exchange), 10.30 (1H, d, NH, *J* = 10, D$_2$O exchange), 12.03 (1H, d, NH, *J* = 10, D$_2$O exchange); MS: *m/z* = 332.37 [M]⁺; analysis: for C$_{16}$H$_{16}$N$_2$O$_4$S, calcd. C 57.82, H 4.85, N 8.43, S 9.65%; found C 57.80, H 4.84, N 8.44, S 9.63 %.

AChE/BChE inhibition studies

ChE inhibitory activities of the new compounds against AChE and BChE were determined by Ellman's method and this method was based on previous studies [38]. Activities of these enzymes were evaluated spectrophotometrically at a wavelength of 412 nm.

Cell culture

Materials

The following materials were used in this study: The cell culture medium (RPMI 1640; Sigma-Aldrich Cat No: R8758, USA), fetal bovine serum (FBS; Sigma-Aldrich Cat No: F7524, USA), %1 penicillin/streptomycin (Sigma-Aldrich Cat No: P4333, USA), L-glutamine (Sigma-Aldrich Cat No: 59202C, USA), trypsin-EDTA solution (Sigma-Aldrich Cat No: 59417C, USA), dimethyl sulfoxide (DMSO) (Sigma-Aldrich Cat No: PHR1309, USA), MTT (3-(4,5-dimethylthiazol-2-yl)-2,5-diphenyltetrazolium bromide; Sigma-Aldrich Cat No: M2128, USA). The culture plates (96 wells) were purchased from Nunc (Brand products, Denmark).

Cell culture

Following cancer and normal cell lines obtained from ATCC and stored in liquid nitrogen were used for the study. A549 (Lung Carcinoma) and Beas-2B (Lung Epithelium Normal) cells were cultured in RPMI-1640 media supplemented with 10% Fetal Bovine Serum (FBS), 100 μg/mL streptomycin/100 IU/mL penicillin in incubators at 37 °C under humid conditions containing 5% CO_2.

Cell viability assay

The cytotoxic effects of all molecules were assessed using the MTT (3-(4,5-dimethylthiazol2-yl)-2,5-diphenyltetrazolium bromide) assay. The cells (A549 and Beas-2B) were incubated in 96-well sterile plates for 24 hours with 1×10^4 cells per well. The media were removed and the molecules were incubated at doses of 0, 2.5, 5, 10, 25, 50, 100, and 200 μg/mL for 24 hours. 10 μL of MTT (0.5 mg/mL) were added into each well as the reactive agent. After 4 hours of incubation, the media was removed and substituted with 100 μL of DMSO, after which measurements were performed at OD_{570}-OD_{690} nm using a plate reader (Thermo Multiskan GO, Thermo, USA). Following these measurements, plots were formed and the IC_{50} value was calculated.

Cell morphology images

After cells were incubated in 12-well plates, 5×10^4 cells per plate, for 24 h, the treatment with IC_{50} doses, was carried out by incubating for 24 h at 37 °C. Morphological changes were assessed using a light microscope (Olympus CKX 51, DP73).

Theoretical methods

Theoretical calculations provide important information about the chemical and biological properties of molecules. Many quantum chemical parameters are obtained from theoretical calculations. The calculated parameters are used to explain the chemical activities of the molecules. Many programs are used to calculate molecules. These programs are Gaussian09 RevD.01 and Gauss View 6.0 [39]. By using these programs, calculations were made in B3LYP, HF, and M06-2x methods with the 6-31++g (d,p) basis set. As a result of these calculations, many quantum chemical parameters have been found. Each parameter describes a different chemical property of molecules, the calculated parameters are calculated as follows [40, 41].

$$\chi = -\left(\frac{\partial \mathrm{E}}{\partial \mathrm{N}}\right)_{v(r)} = \frac{1}{2}(I + A) \cong -\frac{1}{2}(E_{HOMO} + E_{LUMO})$$

$$\eta = -\left(\frac{\partial^2 E}{\partial N^2}\right)_{v(r)} = \frac{1}{2}(I - A) \cong -\frac{1}{2}(E_{HOMO} - E_{LUMO})$$

$$\sigma = 1/\eta \qquad \omega = \chi^2/2\eta \qquad \varepsilon = 1/\omega$$

An important method used to determine the molecules with the highest activity against biological materials is molecular docking. Its calculations are made in Schrödinger's Maestro Molecular modeling platform (version 12.8) [42, 43]. The prepared proteins and molecules interact with each other with the Glide ligand docking tool [44]. Finally, the Qik-prop module of the Schrödinger software was used while performing ADME/T analysis (absorption, distribution, metabolism, excretion, and toxicity to examine the effects of the studied molecules on human metabolism [45].

MM-GBSA calculation

The binding free energy of ligand-protein complexes was found using the MM-GBSA method of the Prime module from Schrodinger. Other parameters were set by default [46]. During the calculation, the OPLS3e force field, VSGB solvent model, and rotamer search algorithms were applied to define the binding free energy. Here, we performed the binding free energy calculations of all complexes with the following equation:

$$\Delta G_{bind} = G_{complex} - (G_{protein} + G_{ligand})$$

where ΔG_{bind} is the binding free energy, $G_{complex}$ ligand-protein complexes are the free energy value, $G_{protein}$ is the target protein's free energy value, and G_{ligand} is the free energy value of the ligand.

CONCLUSION

A novel series of enaminone derivatives of sulfonamides (**1-11**) were synthesized in good yield. All the compounds were characterized and confirmed spectroscopically by ^{1}H NMR and ^{13}C NMR. All the synthesized compounds were screed for choline esterase (ChE) inhibitory activity against AChE and BChE. Compound **9** was found to be the most potent compound for AChE and BChE. All the synthesized compounds were also screened for cytotoxic activity against the lung cancer cell line. The compounds **2** and **10** were found the most potent compounds having cytotoxic effects. The activities of molecules against various proteins were investigated in molecular docking calculations. As a result of ADME/T analysis, it has been observed that the molecules will be good drug candidates.

ACKNOWLEDGMENTS

REFERENCES

1. Cindrić, M.; Rubčić, M.; Hrenar, T.; Pisk, J.; Cvijanović, D.; Lovrić, J.; Vrdoljak, V. Novel enaminones as non-cytotoxic compounds with mild antibacterial activity: Synthesis and structure-activity correlations. *J. Mol. Str.* **2018**, 1154, 636642.

2. Kumar, L.J.; Sarveswari, S.; Vijayakumar, V. DMFDMA catalyzed synthesis of 2(dimethylamino) methylene)-3,4-dihydro-9-arylacridin-1(2H)-ones and their derivatives: in-vitro antifungal, antibacterial and antioxidant evaluations. *Open Chem.* **2018**, 16, 1077-1088.

3. Bangalore, P.K.; Vagolu, S.K.; Bollikanda, R.K.; Veeragoni, D.K.; Choudante, P.C.; Misra, S.; Sriram, D.; Sridhar, B.; Kantevari, S. Usnic acid enaminone coupled 1,2,3-triazoles as antibacterial and antitubercular Agents. *J. Nat. Prod.* **2020**, 83, 26-35.

4. Amaye, I.J.; Heinbockel, T.; Woods, J.; Wang, Z.; Martin-Caraballo, M.; Jackson Ayotunde, P. 6 Hz active anticonvulsant fluorinated N-benzamide enaminones and their inhibitory neuronal activity. *Int. J. Environ. Res. Public Health* **2018**, 15, 1784.

5. Ghorab, M.M.; Ragab, F.A.; Heiba, H.I.; El-Gazzar, M.G.; El-Gazzar, M.G.M. Novel thioureido-benzenesulfonamide derivatives with enaminone linker as potent anticancer, radiosensitizers and VEGFR2 inhibitors. *Bioorg. Med. Chem. Lett.* **2018**, 28, 1464-1470.

6. Kumar, R.; Saha, N.; Purohit, P.; Garg, S.K.; Seth, K.; Meena, V.S.; Dubey, S.; Dave, K.; Goyal, R.; Sharma, S.S.; Banerjee, U.C.; Chakraborti, A.K. Cyclic enaminone as new chemotype for selective cyclooxygenase-2 inhibitory, anti-inflammatory, and analgesic activities. *Eur. J. Med. Chem.* **2019**, 182, 111601.

7. Sowmya, P.V.; Poojary, B.; Revanasiddappa, B.C.; Vijayakumar, M.; Nikil, P.; Kumar, V. Novel 2-methyl-6-arylpyridines carrying active pharmacophore 4,5-dihydro 2-pyrazolines: synthesis, antidepressant, and anti-tuberculosis evaluation. *Res. Chem. Intermed.* **2017**, 43, 7399-7422.

8. Bhat, M.A.; Imran, M.; Khan, S.A.; Siddiqui, N. Biological activities of sulfonamides. *Indian J. Pharm. Sci.* **2005**, 67, 151-159.

9. Azevedo-Barbosa, H.; Dias, D.F.; Franco, L.L.; Hawkes, J.A.; Carvalho, D.T. From antibacterial to antitumour agents: A brief review on the chemical and medicinal aspects of sulfonamides. *Mini. Rev. Med. Chem.* **2020**, 20, 2052-2066.

10. Rehman, H.; Qadir, A.; Ali, Z.; Nazir, S.; Zahra, A.; Shahzady, T.G. Synthesis and characterization of novel sulfonamides derivatives and their antimicrobial, antioxidant and cytotoxicity evaluation. *Bull. Chem. Soc. Ethiop.* **2017**, 31, 491-498.

11. Kavitha, S.; Nasarullah, Z.; Kannan, K. Synthesis and biological evaluation of sulfonamide-based 1,3,4-oxadiazole derivatives. *Bull. Chem. Soc. Ethiop.* **2019**, 33, 307-319.

12. Taslimi, P.; Turhan, K.; Türkan, F.; Karaman, H.S.; Turgut, Z.; Gulcin, I. Cholinesterases, α-glycosidase, and carbonic anhydrase inhibition properties of 1Hpyrazolo [1,2-b] phthalazine-5,10-dione derivatives: Synthetic analogues for the treatment of Alzheimer's disease and diabetes mellitus. *Bioorg. Chem.* **2020**, 97, 103647.

13. Tas, A.; Tüzün, B.; Khalilov, A.N.; Taslimi, P.; Ağbektas, T.; Cakmak, N.K. In vitro cytotoxic effects, in silico studies, some metabolic enzymes inhibition, and vibrational spectral analysis of novel β-amino alcohol compounds. *J. Mol. Str.* **2023**, 1273, 134282.

14. Frisch, M.J.; Trucks, G.W.; Schlegel, H.B.; Scuseria, G.E.; Robb, M.A.; Cheeseman, J.R.; Scalmani, G.; Barone, V.; Mennucci, B.; Petersson, G.A.; Nakatsuji, H.; Caricato, M.; Li, X.; Hratchian, H.P.; Izmaylov, A.F.; Bloino, J.; Zheng, G.; Sonnenberg, J.L.; Hada, M.; Ehara, M.; Toyota, K.; Fukuda, R.; Hasegawa, J.; Ishida, M.; Nakajima, T.; Honda, Y.; Kitao, O.; Nakai, H.; Vreven, T.; Montgomery Jr., J.A.; Peralta, J.E.; Ogliaro, F.; Bearpark, M.; Heyd, J.J.; Brothers, E.; Kudin, K.N.; Staroverov, V.N.; Kobayashi, R.; Normand, J.; Raghavachari, K.; Rendell, A.; Burant, J.C.; Iyengar, S.S.; Tomasi, J.; Cossi, M.; Rega, N.; Millam, J.M.; Klene, M.; Knox, J.E.; Cross, J.B.; Bakken, V.; Adamo, C.; Jaramillo, J.; Gomperts, R.; Stratmann, R.E.; Yazyev, O.; Austin, A.J.; Cammi, R.; Pomelli, C.; Ochterski, J.W.; Martin, R.L.; Morokuma, K.; Zakrzewski, V.G.; Voth, G.A.; Salvador, P.; Dannenberg, J.J.; Dapprich, S.; Daniels, A.D.; Farkas, O.; Foresman, J.B.; Ortiz, J.V.; Cioslowski, J.; Fox, D.J. *Gaussian 09, Revision B.01*, Gaussian Inc.: Wallingford CT; **2010**.

15. Schrödinger Release 2021-3: Maestro, Schrödinger, LLC, New York; **2021**.

16. Becke, A.D. Density-functional thermochemistry. I. The effect of the exchange-only gradient correction. *J. Chem. Phys.* **1992**, 96, 2155-2160.

17. Vautherin, D.; Brink, D.T. Hartree-Fock calculations with Skyrme's interaction. I. Spherical nuclei. *Phy. Rev. C* **1972**, 5, 626.

18. Hohenstein, E.G.; Chill, S.T.; Sherrill, C.D. Assessment of the performance of the M05−2X and M06−2X exchange-correlation functionals for noncovalent interactions in biomolecules. *J. Chem. Theory Comput.* **2008**, 4, 1996-2000.

19. Bhat, M.A.; Al-Omar, M.A.; Naglah, A.M. Synthesis and in vivo anti-ulcer evaluation of some novel piperidine-linked dihydropyrimidinone derivatives. *J. Enzy. Inhib. Med. Chem.* **2018**, 33, 978-988.

20. Eldehna, W.M.; Abo-Ashour, M.F.; Berrino, E.; Vullo, D.; Ghabbour, H.A.; Al-Rashood, S.T.; Hassan, G.S.; Alkahtani, H.M.; Almehizia, A.A.; Alharbi, A.; Abdel-Aziz, H.A. Supuran, C.T. SLC-0111 enaminone analogs, 3/4-(3-aryl-3-oxopropenyl) minobenzenesulfonamides, as novel selective subnanomolar inhibitors of the tumor-associated carbonic anhydrase isoform IX. *Bioorg. Chem.* **2019**, 83, 549-558,

21. Mermer, A.; Bulbul, M.V.; Kalender, S.M.; Keskin, I.; Tuzun, B.; Eyupoglu, O.E. Benzotriazole-oxadiazole hybrid Compounds: Synthesis, anticancer Activity, molecular docking and ADME profiling studies. *J. Mol. Liq.* **2022**, 359, 119264.

22. Poustforoosh, A.; Faramarz, S.; Negahdaripour, M.; Tüzün, B.; Hashemipour, H. Tracing the pathways and mechanisms involved in the anti-breast cancer activity of glycyrrhizin using bioinformatics tools and computational methods. *J. Biomol. Struct. Dyn.* **2023**, 42, 819-833.

23. Kekeçmuhammed, H.; Tapera, M.; Tüzün, B.; Akkoç, S.; Zorlu, Y.; Sarıpınar, E. Synthesis, molecular docking and antiproliferative activity studies of a thiazole-based compound linked to hydrazone moiety. *ChemistrySelect* **2022**, 7, e202201502.

24. Poustforoosh, A.; Hashemipour, H.; Tüzün, B.; Azadpour, M.; Faramarz, S.; Pardakhty, A.; Nematollahi, M.H. The impact of D614G mutation of SARS-COV-2 on the efficacy of anti-viral Drugs: A comparative molecular docking and molecular dynamics study. *Curr. Microbiol.* **2022**, 79, 1-12.

25. Rezaeivala, M.; Bozorg, M.; Rafiee, N.; Sayin, K.; Tuzun, B. A new morpholine based ligand as corrosion inhibitor for carbon steel during acid pickling: Experimental and theoretical studies. *Inorg. Chem. Commun.* **2022**, 148, 110323.

26. Tüzün, B.; Sayin, K.; Ataseven, H. could momordica charantia be effective in the treatment of COVID19. *Cumhuriyet Sci. J.* **2022**, 43, 211-220.

27. Özmen, Ü.Ö.; Tüzün, B.; Ayan, E.B.; Çevrimli, B.S. Eco-friendly and potential colin esterase enzyme inhibitor agent sulfonyl hydrazone series: Synthesis, bioactivity screening, DFT, ADME properties, and molecular docking study. *J. Mol. Str.* **2023**, 1286, 135514.

28. Gao, Y.; Wang, H.; Wang, J.; Cheng, M. In silico studies on p21-activated kinase 4 inhibitors: comprehensive application of 3D-QSAR analysis, molecular docking, molecular dynamics simulations, and MM-GBSA, calculation. *J. Biomol. Struct. Dyn.* **2020**, 38, 4119-4133.

29. Chinnasamy, S.; Selvaraj, G.; Kaushik, A.C.; Kaliamurthi, S.; Chandrabose, S.; Singh, S.K.; Thirugnanasambandam, R.; Gu, K.; Wei, D.Q. Molecular docking and molecular dynamics simulation studies to identify potent AURKA inhibitors: assessing the performance of density functional theory, MM-GBSA and mass action kinetics calculations. *J. Biomol. Struct. Dyn.* **2020**, 38, 4325-4335.

30. Çelik, M.S.; Çetinus, Ş.A.; Yenidünya, A.F.; Çetinkaya, S.; Tüzün, B. Biosorption of Rhodamine B dye from aqueous solution by *Rhus coriaria L.* plant: Equilibrium, kinetic, thermodynamic and DFT calculations. *J. Mol. Str.* **2023**, 1272, 134158.

31. Rbaa, M.; Haida, S.; Tuzun, B.; Hichar, A.; El Hassane, A.; Kribii, A.; Lakhrissi, Y.; Ben Hadda, T.; Zarrouk, A.; Lakhrissi, B.; Berdimurodov, E. Synthesis, characterization and bioactivity of novel 8-hydroxyquinoline derivatives: Experimental, molecular docking, DFT and POM analyses. *J. Mol. Str.* **2022**, 1258, 132688.

32. Chalkha, M.; el Hassani, A.A.; Nakkabi, A.; Tüzün, B.; Bakhouch, M.; Benjelloun, A.T.; El Yazidi, M. Crystal structure, Hirshfeld surface and DFT computations, along with molecular docking investigations of a new pyrazole as a tyrosine kinase inhibitor. *J. Mol. Str.* **2023**, 1273, 134255.

33. Lipinski, C.A. Lead-and drug-like compounds: the rule-of-five revolution. *Drug Discov. Today Technol.* **2004**, 1, 337-341.

34. Lipinski, C.A.; Lombardo, F.; Dominy, B.W.; Feeney, P.J. Experimental and computational approaches to estimate solubility and permeability in drug discovery and development settings. *Adv. drug del. reviews,* **1997**, 23, 3-25.

35. Jorgensen W.J.; Duffy E.M. Prediction of drug solubility from structure. *Adv. drug del. reviews*, **2002**, 54, 355-366.

36. Lennartz, F.; Adams, Y.; Bengtsson, A.; Olsen, R.W.; Turner, L.; Ndam, N.T.; Ecklu-Mensah, G.; Moussiliou, A.; Ofori M.F.; Gamain, B.; Lusingu, J.P.; Petersen, J.E.; Wang, C.W.; Nunes-Silva, S.; Jespersen, J.S.; Lau, C.K.; Theander, T.G.; Lavstsen, T.; Hviid, L.; Higgins, M.K.; Jensen, A.T. Structure-guided identification of a family of dual receptor-binding PfEMP1 that is associated with cerebral malaria. *Cell Host Microbe.* **2017**, 21, 403-414.

37. Bhat, M.A.; Al-Omar, M.A.; Naglah, A.M. Synthesis and in vivo anti-ulcer evaluation of some novel piperidine-linked dihydropyrimidinone derivatives. *J. Enzy. Inhib. Med. Chem.* **2018**, 33, 978-988.

38. Lim do, Y.; Shin, S.H.; Lee, M.H.; Malakhova, M.; Kurinov, I.; Wu, Q.; Xu, J.; Jiang, Y.; Dong, Z.; Liu, K.; Lee, K.Y.; Bae, K.B.; Choi, B.Y.; Deng, Y.; Bode, A.; Dong, Z. A natural small molecule, catechol, induces c-Myc degradation by directly targeting ERK2 in lung cancer. *Oncotarget.* **2016**, 7, 35001-35014.

39. Günsel, A.; Atmaca, G.Y.; Taslimi, P.; Bilgicli, A.T.; Gülçin, İ.; Erdoğmuş, A.; Yarasir, M.N. Synthesis, characterization, photo-physicochemical and biological properties of water-soluble tetra-substituted phthalocyanines: antidiabetic, anticancer and anticholinergic potentials. *J. Photochem. Photobio. A: Chem.* **2020**, 396, 112511.

40. Günsel, A.; Kobyaoğlu, A.; Bilgicli, A.T.; Tüzün, B.; Tosun, B.; Arabaci, G.; Yarasir, M.N. Novel biologically active metallo phthalocyanines as promising antioxidant antibacterial agents: Synthesis, characterization and computational properties. *J. Mol. Str.* **2020**, 1200, 127127.

41. Schrödinger Release 2021-3: LigPrep, Schrödinger, LLC, New York, NY, **2021**.

42. Schrödinger Release 2021-3: Protein Preparation Wizard; Epik, Schrödinger, LLC, New York, NY, **2016**; Impact, Schrödinger, LLC, New York, NY, **2016**; Prime, Schrödinger, LLC, New York, NY, **2021**.

43. Shahzadi, I.; Zahoor, A.F.; Tüzün, B.; Mansha, A.; Anjum, M.N.; Rasul, A.; Irfan, A.; Kotwica-Mojzych, K.; Mojzych, M. Repositioning of acefylline as anti-cancer drug: Synthesis, anticancer and computational studies of azomethines derived from acefylline tethered 4-amino-3mercapto-1,2,4-triazole. *PLoS One* **2022**, 17, e0278027.

44. Schrödinger Release 2021-3: QikProp, Schrödinger, LLC, New York, NY, **2021**.

45. Nayak, A.; Gadnayak, A.; Dash, K. T.; Jena, S.; Ray, A.; Nayak, S.; Sahoo, A. Exploring molecular docking with MM-GBSA and molecular dynamics simulation to predict potent inhibitors of cyclooxygenase (COX-2) enzyme from terpenoid-based active principles of Zingiber species. *J. Biomol. Struct. Dyn.* **2022**, 41, 10840-10850.

46. Chahal, V.; Kakkar, R. A combination strategy of structure-based virtual screening, MM-GBSA, cross-docking, molecular dynamics and metadynamics simulations used to investigate natural compounds as potent and specific inhibitors of tumor linked human carbonic anhydrase IX. *J. Biomol. Struct. Dyn.* **2022**, 41, 5465-5480.